Streamflow Simulation for the Yellow River Basin Using RIEMS and LRM

ZHANG Jingyong*[1] (张井勇), DONG Wenjie[1] (董文杰), FU Congbin[1] (符淙斌),
WU Lingyun[1] (吴凌云), XIONG Zhe[1] (熊 喆), MA Jun[2] (马 骏), and ZHANG Kejia[2] (张克家)

[1] *Global Change System for Analysis, Research and Training Regional Center for Temperate East Asia, Institute of Atmospheric Physics, Chinese Academy of Sciences, Beijing* 100029

[2] *Hydrological Bureau, Yellow River Conservancy Commission, Zhengzhou* 450000

(Received June 24, 2002; revised January 24, 2003)

ABSTRACT

The streamflow over the Yellow River basin is simulated by using the high-resolution Regional Integrated Environmental Model System (RIEMS), and an off-line Large-scale Routing Model (LRM). The RIEMS was designed and has been developed by the Global Change System for Analysis, Research and Training Regional Center for Temperate East Asia (START/TEA) since 1991 and has a good capability to simulate the regional climate of East Asia. The LRM is based on the assumption of linearity and time invariance and can calculate the horizontal travel of water. The RIEMS-LRM allows the direct comparison of predicted and observed streamflow data for large-scale rivers. The application of the RIEMS-LRM to the upper reaches of the Yellow River verifies that the coupled model system has the capability to simulate the streamflow over a large-scale river. Furthermore, the paper discusses the reasons leading to simulation errors.

Key words: RIEMS, LRM, Yellow River, streamflow

1. Introduction

The interactions between atmosphere and hydrology play an important role in the rapidly developing global change science and the opportunity now exists for great progress on the issues due to field experiment data accumulation and numerical modeling development. Current atmospheric general circulation models (GCMs) and numerical weather prediction models coupling with land surface parameterization schemes such as BATS (Dickinson et al., 1986) SiB (Sellers et al., 1986) and LSM (Bonan, 1995) are used to calculate the interface between meteorology and hydrology. But the resolution of GCMs is too coarse to have good capability to reproduce some regional characteristics, so regional climate models (RCMs) have been developed with the aim of enhancing the modeling ability to identify regional features of climate and are coupled with land surface parameterization schemes to simulate regional climate (Giorgi et al., 1993a, b). Over the last 20 years, there has been an explosion of research activity aiming at improving land surface schemes in current GCMs and RCMs (Henderson-Sellers et al., 1995). But much attention in these efforts has been focused on the ability to correctly deal with energy over a range of climate, land surface, and soil moisture characteristics, furthermore, the schemes calculate energy and water fluxes only in the vertical direction, and have not taken any care to preserve the travel time of water in the horizontal direction, so most land surface schemes simulate runoff but not streamflow (Su and Hao, 2001). We cannot accurately evaluate water processes in the models due to the lack of observed runoff and soil water data.

The streamflow is a spatial integrator of hydrological processes and it offers the opportunity to verify the GCM or RCM surface water balance, because the streamflow is the easiest component of the surface water budget to be directly measured. So streamflow simulation for large rivers using a regional climate model, and an off-line large-scale routing model is a good selection.

*E-mail: zjy@tea.ac.cn

In this paper, we focus on simulating the streamflow over the Yellow River basin by using RIEMS with BATS developed in START/TEA, and an off-line LRM from the Department of Hydrological Sciences, University of Arizona. We select the RIEMS because previous works have verified that the RIEMS has good capacity to simulate regional climate and can describe more regional characteristics compared with GCMs (Fu et al., 1998; Fu et al., 2000; Fu, 2001; Wei, 1997; Fu and Yuan, 2001), and BATS can provide more responsive and correctly diurnal outputs of energy and moisture fluxes (Dickinson and Henderson-Sellers, 1988). The large-scale routing model is based on assumptions of linearity and time invariance (Lohmann et al., 1996) and was validated in the Red-Arkansas River basin, and showed good capability of simulating the streamflow (Lohmann et al., 1998). The Yellow River is selected as the test catchment. The paper is organized as follows. Section 2 briefly describes the models, the coupled approach, and experiment design, section 3 compares the simulation results with observed data, and finally in section 4 the conclusions and a summary are given.

2. Models description and approach

2.1 *RIEMS with BATS*

The regional integrated environmental model system (RIEMS) has been under development by START/TEA since 1991. Version 1.0 of RIEMS is based on the efforts made in coupling two major components of a RCM— climate-vegetation interaction and climate-aerosol interaction–which can capture related processes of the "General Monsoon System" which is a coupled physical-chemical-biological-social monsoon system (Fu et al., 2000) and is used in this paper. The dynamical component of the RIEMS is the same as that of the PSU/NCAR meso-scale model MM5 (Grell et al., 1994) and is coupled with BATS 1E and the CCM3 (Kiehl et al., 1996) radiation package, and many physical processes are included in the RIEMS such as a boundary layer scheme, cumulus convection processes, etc. This is a grid-based, hydrostatic, compressible, primitive equation, terrain-following, σ-vertical coordinate model, and the radiation transfer and planetary boundary layer calculations are performed using the CCM3 radiation package and Holtslag planetary boundary layer scheme (Holtslag et al., 1990), respectively.

For the following discussion, it is useful to describe the land surface scheme used in the RIEMS in detail–the biosphere-atmosphere transfer scheme (BATS) (Dickinson et al., 1993). The BATS is designed to describe the role of vegetation and interactive soil moisture in modifying the surface-atmosphere exchanges of momentum, energy, and water vapor. It comprises a vegetation layer, a snow layer, and a three-layer soil water model (a 10 cm thick surface soil layer, 1–2 m thick root zone, and a 5 m thick deep soil layer). Prognostic equations are solved for the soil temperature and water content. In the presence of vegetation, the temperature of canopy air and canopy foliage is calculated diagnostically via an energy balance formulation. The soil hydrology calculations include predictive equations for the water content of all soil layers which account for precipitation, snowmelt, canopy foliage drip, evapotranspiration, surface runoff, infiltration below the root zone, and diffusive exchange of water between soil layers. Sensible heat, water vapor, and momentum fluxes at the surface are calculated by using a standard surface drag coefficient formulation based on surface-layer similarity theory. In version 1E of BATS, 18 vegetation types, 12 soil textures and different soil colors are described for the soil albedo calculation.

The initial soil moisture in the RIEMS-BATS is related with land cover type, depth of total soil at the grid point, fraction of void soil, and fraction of water content.

The runoff is a very important factor in the interactions between atmosphere and hydrology, and is used as the input to the large-scale routing model. So how is the runoff calculation performed in the BATS?

Considering the criteria that there should be small surface runoff at the soil moisture of field capacity and complete surface runoff at saturated soil, the surface runoff R_S is parameterized by:

$$\begin{aligned} R_S &= (\rho_w/\rho_{wsat})^4 G\,, \qquad T_{g1} \geq 0^\circ\mathrm{C} \\ &= (\rho w/\rho_{wsat}) G\,, \qquad T_{g1} < 0^\circ\mathrm{C} \end{aligned}$$

where T_{g1} is surface soil temperature, ρ_{wsat} is the saturated soil water density, and ρ_w is the soil water density weighted toward the top layer, as defined by

$$\rho_w = \rho_{wsat}\frac{(S_1 + S_2)}{2}\,.$$

S_1 and S_2 are respectively defined as

$$S_1 = \frac{S_{rw}}{S_{rwmax}}\,,$$

$$S_2 = \frac{S_{sw}}{S_{swmax}}\,,$$

where S_{rw} is the rooting soil water, and S_{rwmax} is the maximum value of S_{rw}, S_{sw} is the surface soil water, and S_{swmax} is the maximum value of S_{sw}.

G equals the sum of the rainfall and snowmelt minus evaporation. For negative G, $R_S = 0$.

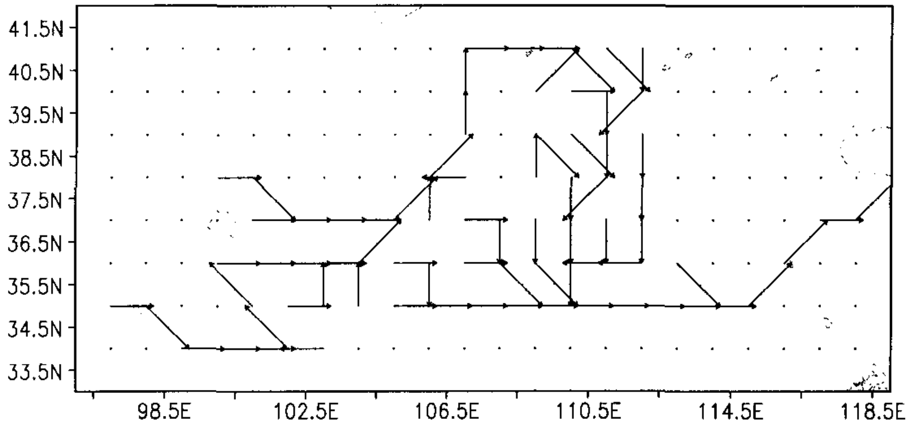

Fig. 1. The $1° \times 1°$ schematic river network for the Yellow River basin.

2.2 *Large-scale routing model* (*LRM*)

The runoff reaching the outlet of a grid box and the transport of water through the river network are calculated in the routing model, and it is assumed that water can leave a grid cell only in the direction of one of its eight neighboring grid cells. Then, the runoff is combined with the river discharge and routed downstream. The runoff calculation is performed using linear and time-invariant models (Lohmann et al., 1996) in the within-grid cell and river routing contributions. A simple baseflow separation technique is used to account for the different timing response of surface and subsurface runoffs. The surface runoff calculation is represented based on the concept of the unit hydrograph (UH), first introduced by Sherman (1932) and further improved in the last decades (e.g., Duband et al., 1993), in each grid cell. This runoff produced in the RIEMS-BATS can be considered as the average value in each grid cell.

River routing in this model is calculated using the linearized Saint-Venant equation (Mesa and Mifflin, 1986; Lettenmaier and Wood 1993; Fread, 1993):

$$\frac{\partial Q}{\partial t} = D\frac{\partial^2 Q}{\partial x^2} - C\frac{\partial Q}{\partial x} .$$

By using measurements or rough estimation from geographical data of the riverbed, we can get the parameters C (wave velocity) and D (diffusivity). One C and one D are used in every grid box, which reflect the main characteristics of the water transport in a river. We constructed an approximate river network using digitized data and Yellow River basin maps and Fig. 1 gives the river network.

2.3 *Basin description*

The Yellow River covers an area of 794712 km^2 including the Erdos inner flow region, and flows through 9 provinces from west to east in China, and ends in the Bohai Sea. The basin lies in the box 32°–42°N and 96°–119°E. The climate ranges from humid, semi-humid conditions in the eastern part of the basin to semiarid and arid conditions in the western part on the whole. Mean annual precipitation varies from more than 1600 mm in the moist areas to less than 200 mm in the driest areas. Precipitation in the basin is summer dominant, much of which is brought from the summer monsoon.

2.4 *Approach and experiment design*

The RIEMS domain includes 151×111 grid points in longitude and latitude with the center at (35°N, 105°E), and covers an area of 9060 km$\times$6660 km. Figure 2 gives the model domain, topography, and the scope of the Yellow River basin. The land cover dataset used in the RIEMS simulation is the land cover classification from global datasets for land-atmosphere models at $1° \times 1°$ resolution (Meeson et al., 1995; DeFries et al., 1994). The topography data with a resolution of 0.5°×0.5° from NCAR is used as the topography situation of the RIEMS. The integral step size is 120 seconds and the horizontal grid point spacing is 60 km in the RIEMS. So the land cover and topography data are interpolated to the resolution. The meteorological initial and lateral boundary conditions necessary to drive the RIEMS were interpolated from the 6 hourly 2.5°×2.5° National Centers for Environment Prediction (NCEP) reanalysis data. The lateral boundary conditions were provided using the relaxation technique with a 10-grid buffer zone.

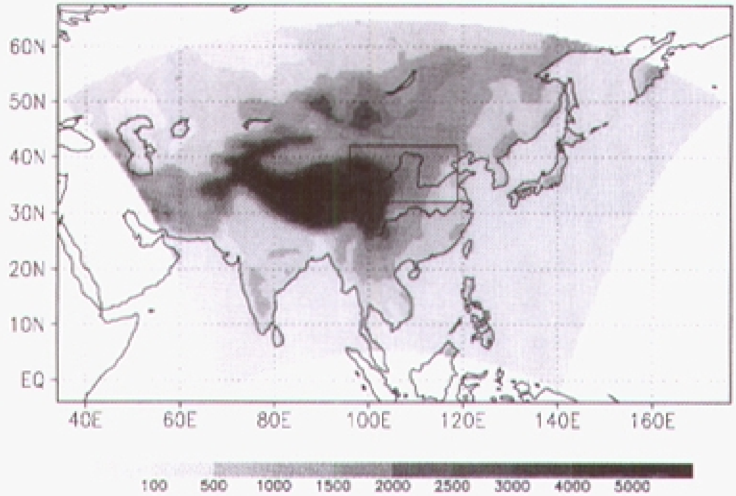

Fig. 2. Model domain (shaded area), topography and the scope of Yellow River basin.

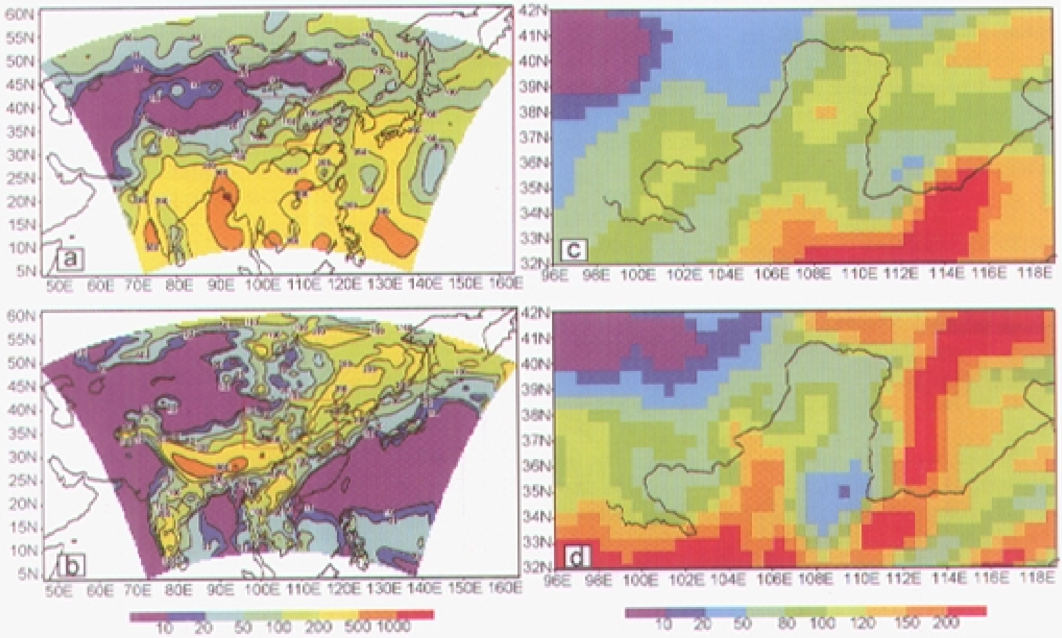

Fig. 3. The observed (a) and simulated (b) total precipitation over model domain, and observed (c) and simulated (d) total precipitation over Yellow River basin in July, 1997 (mm).

The horizontal resolution of the LRM is 1°. The RIEMS was integrated for the period 1 March 1997 to 30 September 1998 with a resolution of 60 km, and the simulated surface runoff using RIEMS from 1 April to 30 September 1997 was interpolated to the $1° \times 1°$ resolution and was used to drive the LRM. The data including the latitude and longitude of hydrological stations, the catchment area, the river network, and C, D, and UH of each grid cell were given to drive the LRM too. The flow velocities C in the LRM were adjusted manually, resulting in values from 1.0 m s^{-1} to 2.0 m s^{-1} for the Yellow River. These values do not represent actual channel velocities, because the travel distance between two grid cells is taken as the distance between their centers. D was from 800 m s^{-1} to 2000 m s^{-1}. The schematized river network for the Yellow River is shown in Fig. 1, and the Yellow River basin was overlain by 75 $1° \times 1°$ grid cells. The integral step size of the LRM is 60 minutes.

3. Experimental results

3.1 *Precipitation*

Figure 3 gives the observed and simulated total precipitation for July 1997. It shows that the RIEMS has simulated the Southwest-Northeast precipitation belt well over the land especially over the Yellow River basin, and the high and low rainfall centers have been represented rather well. But the RIEMS slightly overestimated the precipitation over the land. The RIEMS gives poor simulation over the West Pacific Ocean compared with the observed data.

3.2 *Runoff*

Figure 4 shows the spatial pattern of simulated total surface runoff for July 1997 and January 1998 for the RIEMS with BATS over the Yellow River basin area. The simulated surface runoff pattern has an East-to-West gradient on the whole with a higher surface runoff in the eastern part of the basin in summer (July 1997). The surface runoff values vary from 0.0 mm/month in the western arid portion of the valley to more than 100 mm/month in the eastern humid portion in summer. But the simulated surface runoff value is only about 0.1 mm/month in winter (January 1998) possibly due to the limited ability of the RIEMS in simulating winter runoff. Figure 5 gives the spatial distribution of modeled total surface runoff in April and October 1997. The distribution in spring (April 1997) or autumn (October 1997) has an East-to-West gradient, as it does in summer. But the surface runoff values in spring and autumn, about 0.0–10.0 mm/month, are less than those in summer. This spatial pattern of surface runoff is similar to the precipitation pattern.

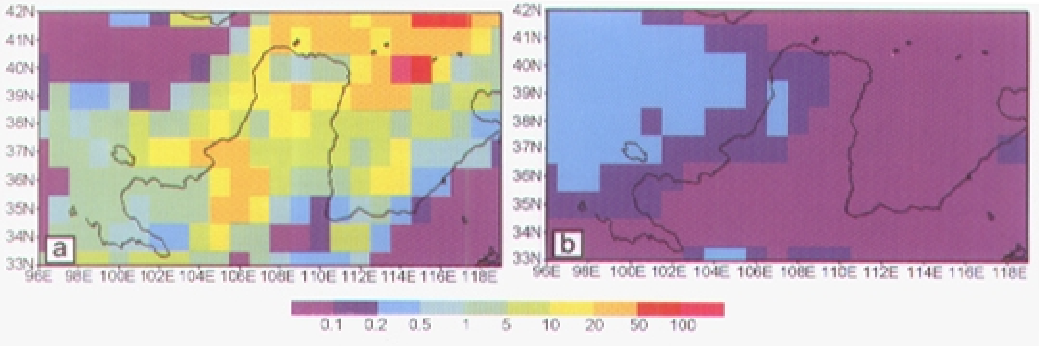

Fig. 4. The spatial pattern of simulated total surface runoff in July, 1997 (a) and January, 1998 (b) (mm/month).

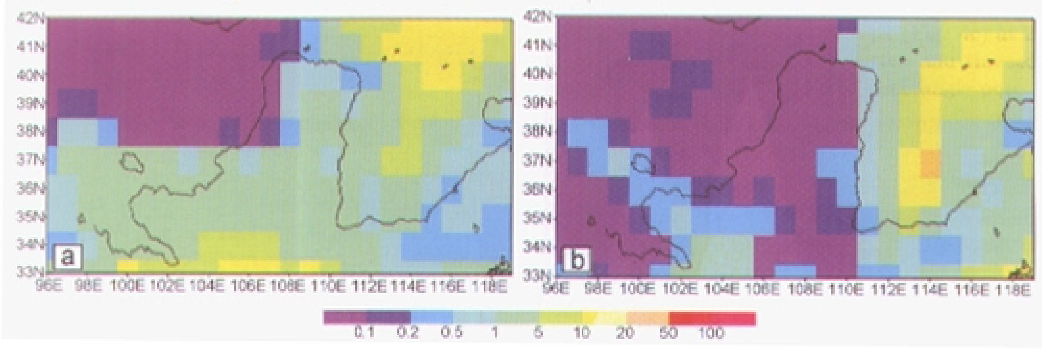

Fig. 5. The spatial distribution of simulated total surface runoff in April (a) and October (b), 1997 (mm/month).

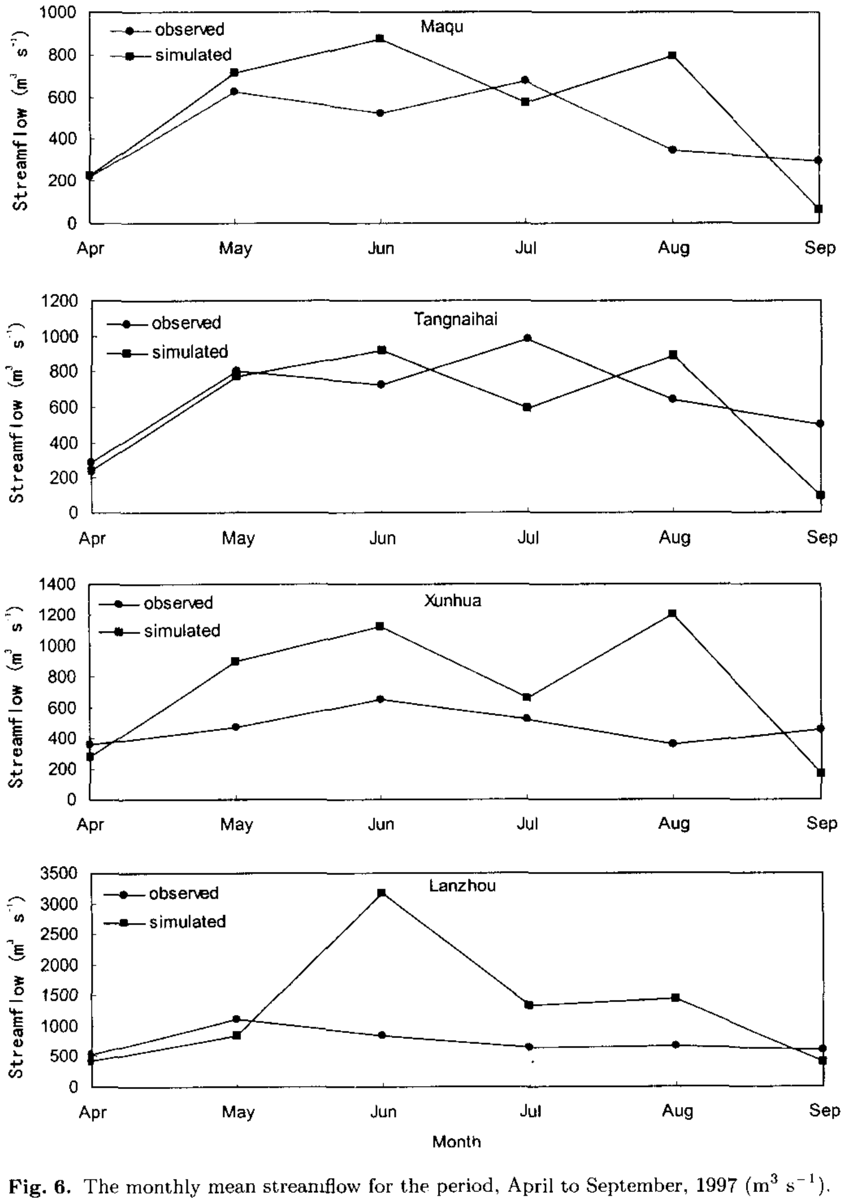

Fig. 6. The monthly mean streamflow for the period, April to September, 1997 (m^3 s^{-1}).

3.3 *Streamflow*

Figure 6 shows the monthly mean streamflow for the period April to September 1997 for four hydrologic stations over the upper reaches of the Yellow River. For the monthly mean distribution, the four locations (Table 1) give different streamflow patterns, but, in general, have the maximum streamflow occurring in June or July. Figure 7 shows the daily mean streamflow for the period from 1 April to 30 September 1997. Simulated streamflow data using the RIEMS-LRM for the Tangnaihai location and Maqu location match the observed streamflow data, both in timing (day and month) and magnitude, and the streamflow at the Maqu location is a little overpredicted. The streamflow at the Xunhua location and Lanzhou location shows a poor fit both in timing and in magnitude

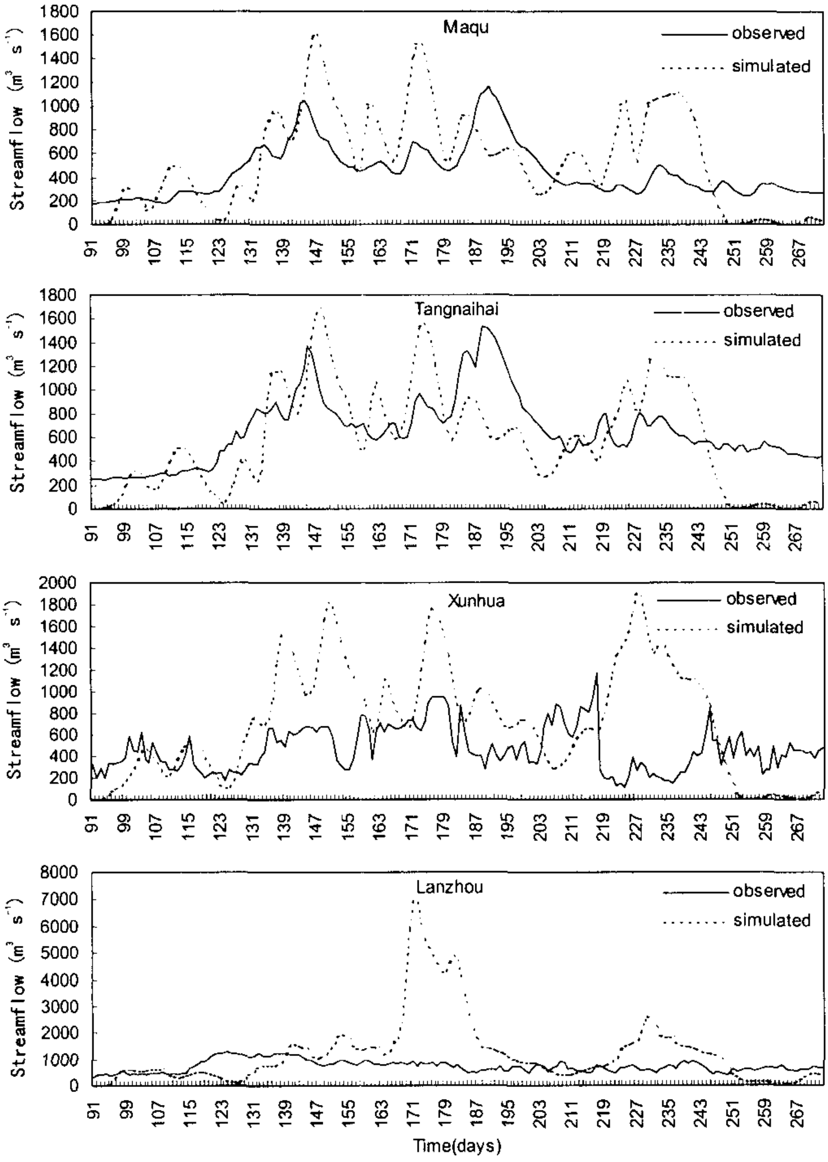

Fig. 7. The daily mean streamflow for the period from 1 April to 30 September, 1997 (m^3 s^{-1}).

compared with the Tangnaihai and Maqu locations not only due to the simulation capability of RIEMS-LRM but also due to the effects of human activities, because there are many reservoirs, dams, and water power stations in the path from the Tangnaihai location to the Lanzhou location. The simulated results will be improved if the streamflow in these parts is naturalized (i.e., with the effects of the dams numerically removed).

In all cases, performance is evaluated by the correlation coefficients between daily mean modeled and observed streamflow. Table 1 gives the true longitude

Table 3. The true longitude and latitude, the longitude and latitude in the RIEMS LRM, and correlation coefficients of ten locations in the upper Yellow River

	Huanghe yan	Jimai	Jungong	Maqu	Tangnai hai	Guide	Xunhua	Xiaochuan	Shangquan	Lanzhou
Longitude(degree)	98.10	99.39	100.39	102.05	100.09	101.24	102.30	103.20	103.18	103.49
Latitude(degree)	34.53	33.46	34.42	33.58	35.30	36.02	35.50	35.56	36.04	36.04
Longitude in RIEMS-LRM(degree)	98.5	99.5	101.5	101.5	101	101.5	102.5	103.5	103.5	103.5
Latitude in RIEMS-LRM(degree)	34.5	34	34	34.5	35.5	36	36	36	36	36
Correlation coefficient between daily mean modeled and observed streamflow	0.43	0.26	0.51	0.57	0.57	0.14	0.16	0.23	0.20	0.11

and latitude, the longitude and latitude in the RIEMS-LRM, and the correlation coefficients of ten locations over the upper Yellow River. In the part above the Tangnaihai location (including the Tangnaihai location), the correlation coefficients between simulation and observation for the locations range from 0.26 to 0.57 with all but two of them above 0.50, and all are significant at the 1% level. For a site such as Huangheyan, which collects runoff from a small area, the edge effects are relatively important. This can result in a relatively small correlation coefficient (for example Huangheyan location, 0.43) than a location such as the Tangnaihai location with a large area for collecting runoff. But in the part from the Tangnaihai location to the Lanzhou location (including the Lanzhou location), the correlation coefficients for five locations (Guide, Xunhua, Xiaochuang, Shangquan, and Lanzhou) are less, 0.14, 0.16, 0.23, 0.20, 0.11, respectively, not only due to the limitation of RIEMS-LRM simulation capability but also due to the effects of human activities.

The biases occurred in all locations of the upper Yellow River, and the reasons possibly include: (1) The parameters in the LRM such as UH need to be adjusted further. In addition, the LRM requires that each grid cell flow in only one direction, and thus each cell has to be assigned to one subbasin or another. This can result in relatively large errors especially in the arid region. (2) The problems in simulating regional climate using the RIEMS are possibly related to land surface scheme, snow and sea ice treatment, longwave radiation, convection schemes, lateral boundary treatment, soil moisture initialization and microphysics of precipitation, etc, and there are a number of uncertainties in regional climate simulation. So more modeling tests should be applied to study them in detail. (3) The human-made changes for water use are important factors to bring a large error to the simulated results. By comparing simulation capacity in the part above the Tangnaihai location with that in the part from the Tangnaihai to Lanzhou locations, the effects of human activities have been analyzed above. (4) The Fleming precipitation-runoff scheme is used in the BATS, and it can simulate runoff not only in the humid regions but also in the arid ones. But the applicability of the scheme in the upper Yellow River needs to be further verified.

4. Discussion and summary

The streamflow of the upper Yellow River (1° grid scale) is simulated using RIEMS-LRM in this paper. The main results include:

(1) The RIEMS-LRM is capable of reproducing the streamflow for the part above the Tangnaihai location of the Yellow River, compared with observed streamflow data. In this part, the correlation coefficients between simulation and observation for five locations (Huangheyan, Jimai, Jungong, Maqu, and Tangnaihai) are 0.43, 0.26, 0.51, 0.57, 0.57, respectively, with all significant at the 1% level.

(2) The RIEMS-LRM shows limited capacity to simulate the streamflow for the part from the Tangnaihai location to the Lanzhou location, compared with the part above the Tangnaihai location, not only due to the limitation of RIEMS-LRM but also due to human-made changes for water use.

The simulation errors are possibly related to the problems of simulating regional climate, the effects of human activities, the applicability of the precipitation-runoff scheme of BATS in the upper Yellow River, and parameter adjustment in the routing model. Suggestions for correcting these are given as follows. (a) RIEMS can be further improved to advance the simulation capacity for regional climate. (b) The naturalized streamflow data can remove the effects of reservoirs and diversions, so the effects of human-made changes can be partly removed if the naturalized data are used. Furthermore, if a model of human-made water use changes is designed and coupled with RIEMS-LRM, the simulated results will better match the observed streamflow data. (c) More offline modeling tests using the BATS could verify the precipitation-runoff scheme and improve it. (d) The parameters of the routing model need to be further adjusted.

We note the water processes such as surface runoff on the current scale of GCMs or RCMs are difficult to verify due to the absence of a detailed global hydrological dataset, even in the near future. The RIEMS-LRM allows the inclusion of observed streamflow data as a verification for the RIEMS. The simulated results for the upper Yellow River demonstrate the feasibility of the RIEMS-LRM for simulating streamflow for large-scale catchments.

In the near future, runs of the RIEMS-LRM with consideration of human-made changes and improvement of other processes will be performed for the complete Yellow River basin.

Acknowledgments. The authors would like to thank the two anonymous reviewers for their valuable suggestion and comments. This work was supported jointly by the National Key Basic Research Development Program (Grant No. G1999043408), the Key Innovation Project of CAS (Grant No. ZKCX2-SW-210, KZCX3-SW-218), and the Western Project of CAS.

REFERENCES

Bonan, G. B., 1995: Land-Atmosphere CO_2 exchange simulated by a land surface process model coupled to an atmospheric general circulation model. *J. Geophys. Res.*, **100**, 2817–2831.

DeFries, R. S., and J. R. G. Townsend, 1994: NDVI-derived land cover classification at global scales. *Int. J. Remote Sens.*, **15**, 3567-3586.

Dickinson, R. E., and A. Henderson-Sellers, 1988: Modeling tropical deforestation: A study of GCM land-surface parameterizations. *Quart. J. Roy. Meteor. Soc.*, **114**, 439–462.

Dickinson, R. E., A. Henderson-Sellers, and P. J. Kennedy, 1993: Biosphere-Atmosphere Transfer Scheme (BATS) version 1e as coupled to the NCAR community Climate Model. Tech. Note. NCAR/TN-387+STR, National Center for Atmospheric Research, Boulder, CO, 72pp.

Dickinson, R. E., A. Henderson-Sellers, P. J. Kennedy, and M. F. Wilson, 1986: Biosphere-Atmosphere Transfer Scheme (BATS) for the NCAR CCM. NCAR/TN-275-STR, Boulder: National Center for Atmospheric Research.

Duband, D., C. Obled, and J. Y. Rodriguez, 1993: Unit hydrograph revisited: An alternate iterative approach to UH and effective precipitation identification. *J. Hydrol.*, **150**, 115–149.

Fread, D. L., 1993: Flow routing. *Handbook of Hydrology*, ch. 10, D. R. Maidment, Ed., McGraw Hill, 10.1–10.36.

Fu Congbin, 2001: Regional climate model inter-comparison project for Asia: Summary for phase one. Proceedings of workshop of APN project #2001-05: Regional climate model inter-comparison project (RMIP) for Asia (phase 1), December 11-14, 2001, Kobe, Japan, 1-11.

Fu Congbin, Wei Helin, and Qian Yun, 2000: Documentation on a Regional Integrated Environmental Model System(RIEMS, version 1). TEACOM Science Report, No. 1, Start Regional Committee for Temperate East Asia, Beijing, 38pp.

Fu Congbin, Wei Helin, Chen Ming, Su Bingkai, Zhao Ming, and Zheng Weizhong, 1998: Simulation of evolution of summer monsoon rainbelts over Eastern China from a regional climate model. *Scientia Atmospherica Sinica*, **22**, 522–534. (in Chinese)

Fu Congbin, and Yuan Huiling, 2001: A virtual numerical experiment to understand the impacts of recovering natural vegetation on the summer climate and environmental conditions in East Asia. *Chinese Science Bulletin*, **46**, 1199–1203.

Giorgi, F., M. R. Marinucci, and G. T. Bates, 1993a: Development of a second generation regional climate model (RegCM2). Part I: Boundary layer and radiative transfer processes. *Mon. Wea. Rev.*, **121**, 2794 2813.

Giorgi, F., M. R. Marinucci, and G. De Canio, 1993b: Development of a second generation regional climate model (RegCM2). Part II: Cumulus cloud and assimilation of lateral boundary conditions. *Mon. Wea. Rev.*, **121**, 2814–2832.

Grell, G., J. Dudhia, and D. R. Stauffer, 1994: A description of the fifth generation Penn State/NCAR mesoscale model(MM5). NCAR Technical Note TN-397+IA, Mesoscale and Microscale Meteorology Division, NCAR, Boulder CO, January 1994, 138pp.

Henderson-Sellers, A., A. J. Pitman, P. K. Love, P. Irrannejad, and T. H. Chen, 1995: The project for inter-comparison of land-surface parameterization schemes (PILPS): Phases 2 and 3. *Bull. Amer. Meteor. Soc.*, **94**, 489–503.

Holtslag, A. A. M., E. I. F. De Bruijn, and H. -L. Pan, 1990: A high resolution air mass transformation model for short-range weather forecasting. *Mon. Wea. Rev.*, **118**, 1561–1575.

Kiehl, J. T., J. J. Hack, G. B. Bonan, B. A. Boville, B. P. Briegleb, D. L. Williamson, and P. J. Rasch, 1996: Description of the NCAR Community Climate Model (CCM3). NCAR/TN-420+STR, NCAR, Boulder, CO, 152pp.

Lettnmaier, D., and E. Wood, 1993: *Handbook of Hydrology*: Hydrologic forecasting. Chap. 26. McGraw-Hill, 26.1–26.30.

Lohmann, D., and Coauthors, 1998: The project for inter-comparison of land-surface parameterization schemes (PILPS) phase 2(c) Red-Arkansas River basin experiment: 3. Spatial and temporal analysis of water fluxes. *Global and Planetary Change*, **19**, 161–179.

Lohmann, D., R. Nolte-Holube, and E. Raschke, 1996: A large-scale horizontal routing model to be coupled to land surface parameterization schemes. *Tellus*, **48A**, 708–721.

Mesa, O. J., and E. R. Mifflin, 1986: On the relative role of hillslope and network geometry in hydrologic response. *Scale Problems in Hydrology*, V. K. Gupta, I. Rodriguez-Iturbe and E. F. Wood Eds., D. Reidel Publishing Company, 1–17.

Meeson, B. W., F. E. Corprew, and J. M. P. McManus, 1995: ISLSCP Initiative I-Global Data Sets for Land Atmosphere Models. 1987-1988, Vol.1–5, published on CD by NASA (GDAAC, ISLSCP, 001-USA).

Sellers, P. J., Y. Mintz, Y. C. Sud, and A. Dalcher, 1986: A simple biosphere model (SiB) for use within general circulation models. *J. Atmos. Sci.*, **43**(6), 505–531.

Sherman, L. K., 1932: Streamflow from rainfall by the unit hydrograph method. *Eng. News. Rec.*, 108, 501–505.

Su Fengge, and Hao Zhencun, 2001: Review of land-surface hydrological processes parameterization. *Advance in Earth Sciences*, **16**(6), 795–801. (in Chinese)

Wei Helin, 1997: Regional climate model and its simulation study of East Asia climate. PhD dissertation, Institute of Atmospheric Physics, Chinese Academy of Sciences, 72pp.

利用RIEMS-LRM对黄河河川径流的模拟研究

张井勇　董文杰　符淙斌　吴凌云　熊喆　马骏　张克家

摘　要

P33 A

利用区域系统环境集成模式(RIEMS) 和一个offline的大尺度汇流模型(LRM) 对黄河的河川径流做了模拟。中国科学院大气物理所东亚中心从1991年开始建立和发展RIEMS，并验证RIEMS对东亚区域气候有较好的模拟能力。LRM是以线性时基不变假定为基础并能够计算水的水平传输的数学模型。RIEMS-LRM可以用来模拟和预测大尺度河流的河川径流。RIEMS-LRM在黄河上游河段的应用证实其有能力对大尺度河流的河川径流进行模拟。此外，作者还分析了模拟误差产生的原因。

关键词：RIEMS，LRM，黄河，河川径流